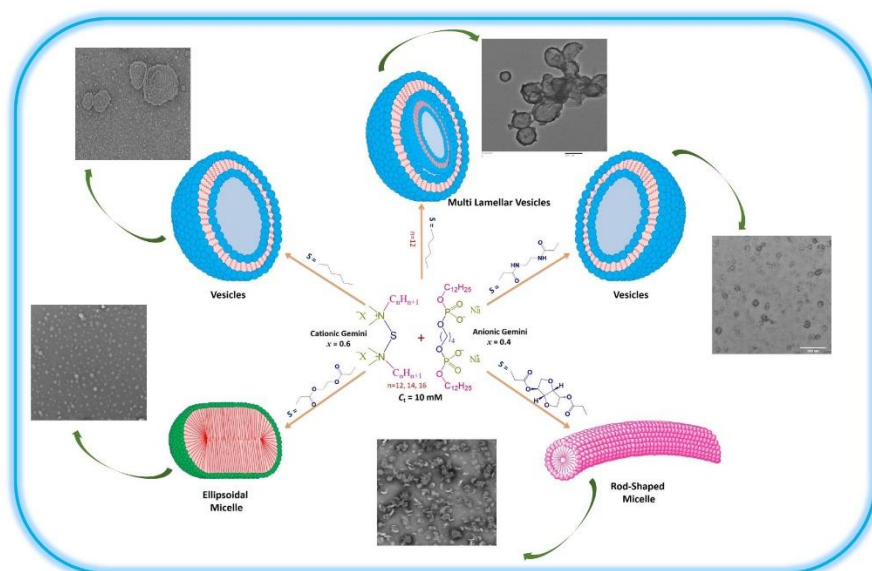


# Chapter 6

## Structural Modification In Self-Assembly of Aqueous Oppositely Charged Mixed Gemini Surfactants



Part of work published in *J. Phys. Chem. B*, 2017, 121, 8756–8766.

& *J. Mol. Liq.* 2019, 279, 108-119.

## 6.1. Introduction

Self-assembly of molecules plays a decisive role in physico-biochemical processes [1]. One of such examples is photosynthesis which involves self-assembly responsible for photophosphorylation [2]. The self-assembly can be considered as a first step for the physical synthesis of an organized structure such as *vesicles*. They have been considered as precursors of the living cell [3, 4]. A rich diversity of amphiphilic molecules (*e.g.* Surfactant) and ways of interaction among them result in self-assembled aggregates like micelles, reverse micelles, vesicles, gels among others [5]. Vesicles have been of interest due to their utility in diverse technologies [6-10] Nature of surfactant molecules is one of the governing factors for the formation of vesicles [11,12].

In recent years, much attention has been paid to cationic surfactants due to their high affinity to negatively charged hydrophobic solutes (nucleotides units of DNA, cell membrane and drugs) [13,14]. It has been reported that catanionic vesicles (formed by the mixing of oppositely charged surfactants) have various advantages over conventional lipid vesicles [11, 15, 16]. Vesicle formation has also been reported when a single/ double chain [17, 18] cationic surfactant (with simple salt) has been mixed to certain medium to higher chain length alcohols [19-21]. Cationic surfactant gives vesicular aggregates in the presence of oppositely charged hydrotropic ions which converts into other morphologies on varying the composition [22].

In this direction, much of the research is now shifted towards mixing a gemini surfactant with a single chain conventional one [23-27]. However, not many reports are available on the mixtures of gemini surfactants [28-30]. As mentioned in earlier chapters (**Chapter 4 and 5**), gemini surfactants are known for better properties such as

lower cmc, higher surface activity, and unusual rheology [27-29, 31-33]. Even then, only a few reports are available related to the influence of nature of spacer on the applications and solution behavior of gemini surfactants [26, 34-44]. However, scanty reports are available in the literature on micellar morphology formed by the mixing of oppositely charged gemini surfactants [29, 45]. This may be due to the fact that such mixtures may result in precipitation, instability or loss of surface activity. This may be due to the interaction between two head groups together with Coulombic charge neutralization. Moreover, the advantages of such systems are not fully exploited. These facts inspired to mix two oppositely charged gemini components and see the variation in the structure of self-assembly so formed with varied composition.

The study constitutes morphological characterization of gemini mixtures and establishes a correlation of mixed assemblies with the nature of the spacer/composition, aggregate charge. Micellar structural information has been collected from Dynamic light scattering (DLS), Transmission Electron Microscopy (TEM) and Small Angle Neutron Scattering (SANS). The charge on mix aggregate has also been acquired by SANS and Zeta potential measurements. It may be mentioned here that phase study of a few systems depicts color changes which hint towards morphological transitions without any visible phase separation. Based on the above morphological studies, samples were selected for the influence of temperature variation. Data show the formation of quite stable structures with minimum variation in self-assembly. For the purpose, various structural variation in geminis are adopted: effect of alkyl tail length; effect of spacer nature; chain-length compatibility effect and influence of heating.

## 6.2. Results and Discussion

### 6.2.1. Structural Evaluation for Individual Aqueous Gemini Surfactants

SANS spectra ( $d\Sigma/d\Omega$  vs  $Q$ ) for 10mM gemini surfactant solution are depicted in Figure 1(a-c). Figure 1 shows interaction peak in all cases which is an indication of the presence of charged micelles in the solution. The related analyzed micellar parameter data for each gemini surfactants are compiled in Table 1. SANS analysis shows that ellipsoidal micelles are present in the solution with every gemini surfactant except 16-4-16. With the dodecyl chain in cationic geminis as well as in 12-4-12A, it is obvious that micelles of higher sphericity will form as reported with another ionic surfactant of the dodecyl chain [46]. For equal alkyl tail length (16 C- atom) gemini with polymethylene spacer of (4 C atom) forms rod-shaped micelles while ellipsoidal morphology observed with geminis having other spacers (Table 1). However, cationic geminis with 14 or 12 C atoms (even anionic also) form only ellipsoidal micelles. This clearly indicates that both spacer and chain-length play equally important role to dictate the type of the morphology. Since polymethylene spacer geminis (16-4-16, 14-4-14 and 12-4-12) are distinctly hydrophobic in comparison to other geminis and, therefore, one can expect increased hydrophobic interactions and aggregate of higher size/morphology. This indeed was observed from the present study (Table 1). Analyzed data can be used to compute the number density of the micelles and hence the average inter-micellar distance ( $D$ ). This can be used to back-calculate the position of the expected correlation peak using equation (given in **Chapter 2, 2.5.9.**) and is found in fairly good agreement with that of experimental one (Figure 1).

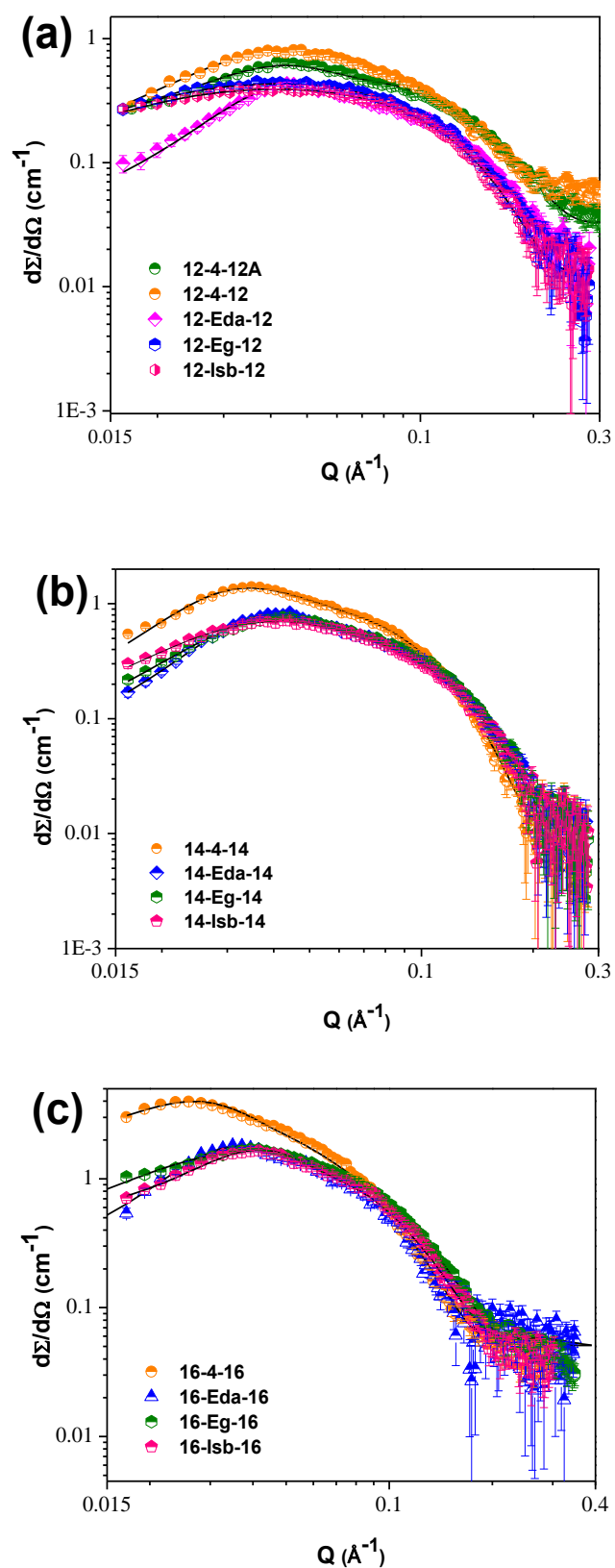


**Figure 1.** SANS spectra of 10 mM pure gemini surfactants at 303 K.

**Table 1.** Micellar dimensions and charge ( $\alpha$ ) for 10 mM aqueous gemini surfactant at 303 K

Surfactant	Semi-major axis $a$ (Å)	Semi-minor axis $b$ (Å)	Fractional charge ( $\alpha$ )	$a/b$	Morphology
12-4-12A	29.5	14.1	0.65	2.1	Ellipsoidal
12-4-12	30.0	16.3	0.53	1.8	Ellipsoidal
12-Eda-12	23.3	15.4	1.06	1.5	Ellipsoidal
12-Eg-12	27.9	15.4	0.31	1.8	Ellipsoidal
12-Isb-12	24.8	16.6	0.28	1.5	Ellipsoidal
14-4-14	36.3	19.7	0.59	1.8	Ellipsoidal
14-Eda-14	29.9	16.9	0.99	1.8	Ellipsoidal
14-Eg-14	28.1	17.1	0.75	1.6	Ellipsoidal
14-Isb-14	30.2	17.1	0.59	1.8	Ellipsoidal
16-4-16	95.8	20.4	0.10	4.7	Rod
16-Isb-16	37.2	20.0	0.43	1.9	Ellipsoidal
16-Eda-16	35.0	20.5	0.21	1.7	Ellipsoidal
16-Eg-16	34.7	17.9	0.09	1.9	Ellipsoidal

### 6.2.2. Structural Evaluation for Mixed Oppositely Charged Gemini Surfactants

The visual appearance of typical gemini mixture (12-4-12A +12-4-12), as a function of composition, is shown in Figure 2. Color changes (clear to bluish to clear) indicate morphological transitions from one microstructure to another induced by composition variation. The appearance of bluish tinge reflects the formation of vesicular aggregates [22].

Mixing of anionic/cationic geminis, in aqueous solution, results in strong coulombic attraction together with hydrophobic interactions among the hydrocarbon tails. The coulmbic effects causes decrease in area of the head group(s) while hydrophobic interactions may cause increase in volume of the alkyl tail part (of the

resulting surfactant moiety produced due the mixing of two gemini components) [47]

Surfactant parameter,  $P (= V/a_0l_c$ ,  $v$  is the volume of the hydrocarbon part of the surfactant(s) molecule(s),  $l_c$  and  $a_0$  are lengths and effective surface area per surfactant(s) molecule(s), respectively), can be related to aggregate morphology [48].

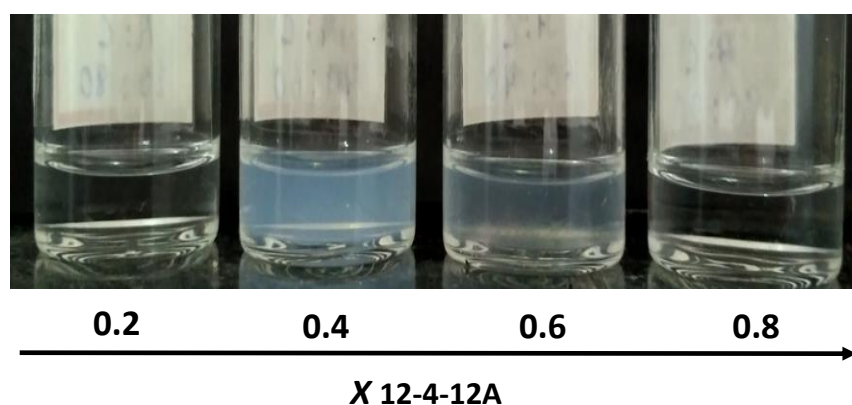


**Figure 2.** Physical appearance of aqueous 12-4-12A + 12-4-12 mixtures as a function of composition (total [surfactant] = 10 mM)

The presence of oppositely charged surfactants has a strong chance to get incorporated in the mixed micelle together with overcoming of electrostatic repulsion. Coulombic attraction can be responsible for the lowering of  $a_0$  with a concomitant increase in  $P$ . Another contribution of the increase in  $P$  comes from by considering two gemini surfactant components of the mixture as a *single amphiphilic moiety* of higher alkyl tail volume ( $V$ ). Various morphological transitions have been explained on the basis of the  $P$  value [49]. Mixing oppositely charged amphiphilic molecules is a promising strategy for the physical synthesis of self -assembly of desired morphology [16, 22].

The idea of coulombic attraction variation can be taken from Zeta ( $\zeta$ ) – potential profiles (for a few systems) obtained with the variation of the composition of the mixture (Figure 3). The crossover of sign (from positive to negative) of  $\zeta$  hints in the

variation of micellar surface charge (as well as  $a_0$  value) which can be correlated with the  $P$  value and the resulting micellar structure produced in the solution is dependent on the mole fraction of each component and decides micellar surface charge which can be related to the variation of  $P$  and hence to the micellar morphology as mentioned above.

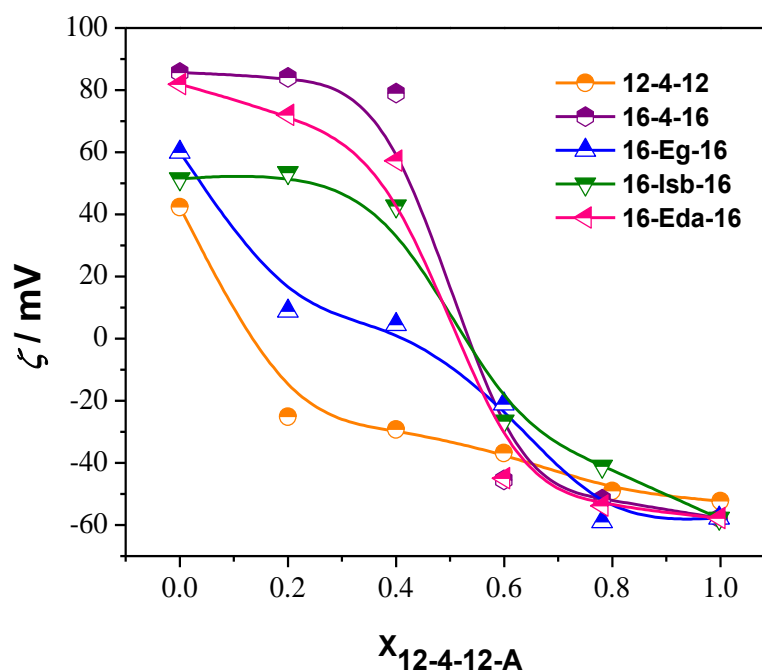


**Figure 3.** Zeta ( $\zeta$ ) – potential data of 10 mM mixed gemini surfactant aqueous systems at a different mole fraction of anionic gemini surfactant ( $x_{12-4-12A}$ ) in aqueous solution at 303 K.

SANS spectra for various compositions of mixed geminis are shown in Figures 4-6. With the addition of anionic 12-4-12A to cationic geminis (keeping total [gemini(s)] constant, 10 mM), interaction peak corresponding to the charged micelle starts disappearing (plateau formation) followed by no plateau in the comparable mole fractions of the two components (0.4 and 0.6, 0.5 and 0.5 or 0.6 and 0.4). At some specific mole fractions (e.g. 0.6/0.4 or 0.4/0.6) of oppositely charged surfactants, the formation of large aggregates with lower charge (rod-like micelles or vesicles) leads to

a reduction in number density and hence increase in inter micellar distance. These systems, therefore, behave as a dilute solution and responsible for the disappearance of the correlation peak in the Q range of the measurements. Also, at approximately equimolar concentrations, there may be near charge balance of the aggregate (of mixed oppositely charged surfactants), making the aggregate nearly pseudo nonionic (as observed by zeta potential data, Figure 3). This restricts the determination of any S(Q) parameters for these concentrations. On comparing the SANS data (Tables 3-5), it is clearly observed that the nature of spacer and alkyl chain-length have distinct effects on SANS parameters of mixed oppositely charged gemini surfactants. The trend of data with 16-Isb-16 (in the mixture) matches with 16-Eg-16 (in the mixture) while the data of 16-4-16 are similar to the data of 16-Eda-16. The behavior was repeated even with geminis of 14C chain (Table 4). In all the above-mentioned mixtures, compositions are more or less similar to the difference of the nature of the spacer. 16- Isb/Eg-16 (or 14-Isb/Eg-14) and 16-4/Eda-16 (or 14-4/Eda-14) fall into two separate groups of forming different kind of morphologies at an individual composition (ellipsoidal/ rod and rod/vesicles). Isb or Eg are distinctly polar spacers than Eda or polymethylene (hydrophobic spacers).

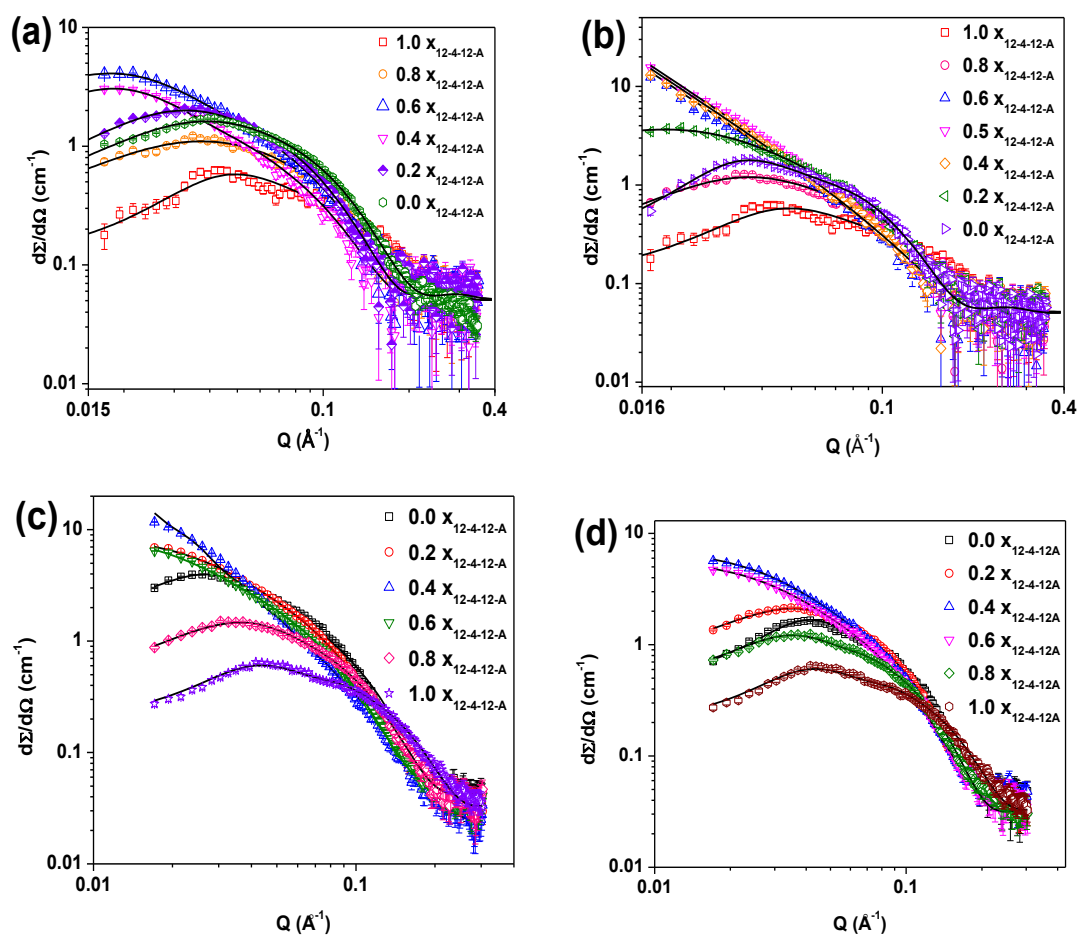


**Figure 4.** SANS spectra of 10 mM mixed aqueous gemini surfactant systems at different mole fraction of anionic gemini surfactant ( $X_{12-4-12A}$ ) at 303 K: (a) 16-Eg-16; (b) 16-Eda-16 (c) 16-4-16 and (d) 16-Isb-16.

**Table 2.** SANS fitted micellar parameters of 10 mM aqueous mixed gemini surfactant systems at 303 K

$x_{12-4-12A}$	Semi-major axis $a$ (Å)	Semi-minor axis $b$ (Å)	Fractional charge ( $\alpha$ )	Aggregation Number
<b>16-Eda-16</b>				
0.0	35.0	20.5	0.21	67
0.2	89.3	20.3	0.04	171
0.4	Vesicles with a bi-layer thickness of 23 Å.			
0.5	Vesicles with a bi-layer thickness of 25 Å.			
0.6	Vesicles with a bi-layer thickness of 22 Å.			
0.8	36.5	20.5	0.10	86
1.0	29.5	14.1	0.65	35
<b>16-Eg-16</b>				
0.0	34.7	17.9	0.09	66
0.2	43.7	20.3	0.09	86
0.4	112.4	20.3	0.04	234
0.6	124.3	20.4	0.03	258
0.8	37.9	16.6	0.10	59
1.0	29.5	14.1	0.65	35
<b>16-4-16</b>				
0.0	95.8	20.4	0.1	182
0.2	111.8	20.3	-	191
0.4	Vesicles with a bi-layer thickness of 25 Å			
0.6	141.2	21.7	-	354
0.8	44.5	19.0	0.18	90
1.0	29.5	14.1	0.65	35
<b>16-Isb-16</b>				
0.0	37.2	20.0	0.43	68
0.2	45.8	20.8	0.16	95
0.4	104.0	20.0	-	210
0.6	101.2	20.0	-	215
0.8	32.3	18.6	0.6	63
1.0	29.5	14.1	0.65	35

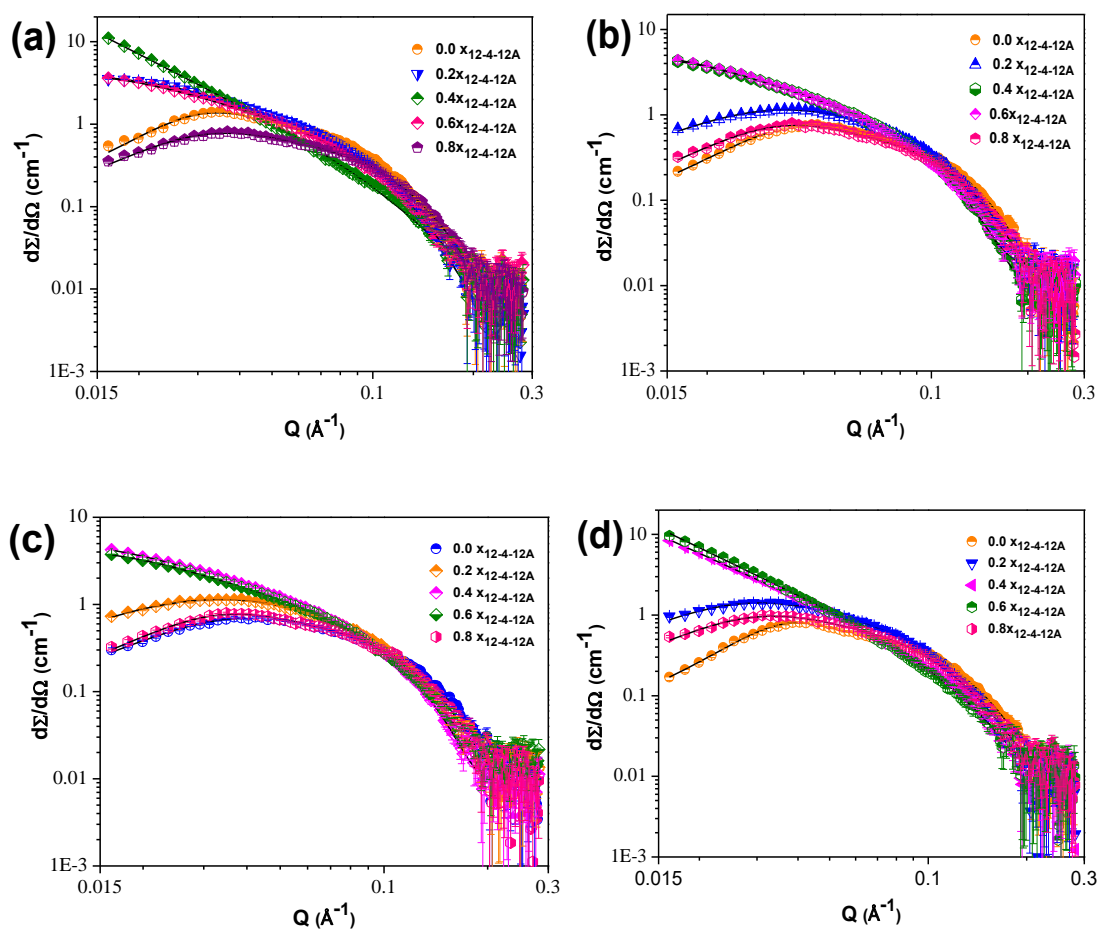


**Figure 5.** SANS spectra of 10 mM mixed aqueous gemini surfactant systems at different mole fraction of anionic gemini surfactant ( $x_{12-4-12A}$ ) at 303 K: (a) 14-4-14; (b) 14-Eg-14 (c) 14-Isb-14 and (d) 14-Eda-14.

**Table 3.** SANS fitted micellar parameters of 10 mM aqueous mixed gemini surfactant systems at 303 K

$x_{12-4-12A}$	Semi-major axis $a$ (Å)	Semi-minor axis $b$ (Å)	Fractional charge ( $\alpha$ )	Aggregation Number
<b>14-Eda-14</b>				
0.0	29.9	16.9	0.99	39
0.2	46.6	19.2	0.29	91
0.4	<b>Vesicles with a bi-layer thickness of 31.0 Å</b>			
0.6	<b>Vesicles with a bi-layer thickness of 31.0 Å</b>			
0.8	37.7	18.41	0.38	74
1.0	29.5	14.1	0.65	35
<b>14-Eg-14</b>				
0.0	28.1	17.1	0.75	40
0.2	38.3	19.3	0.29	76
0.4	145.0	21.2	-	357
0.6	152.4	22.0	-	415
0.8	31.1	17.7	0.5	56
1.0	29.5	14.1	0.65	35
<b>14-4-14</b>				
0.0	36.3	19.7	0.59	64
0.2	108.7	20.6	-	786
0.4	<b>Vesicles with a bi-layer thickness of 30.4 Å</b>			
0.6	131.9	20.8	-	321
0.8	31.7	17.6	0.51	57
1.0	29.5	14.1	0.65	35
<b>14-Isb-14</b>				
0.0	30.2	17.1	0.59	40
0.2	39.9	19.6	0.26	81
0.4	154.4	21.0	-	373
0.6	138.8	20.5	-	328
0.8	30.7	18.1	0.5	58
1.0	29.5	14.1	0.65	35

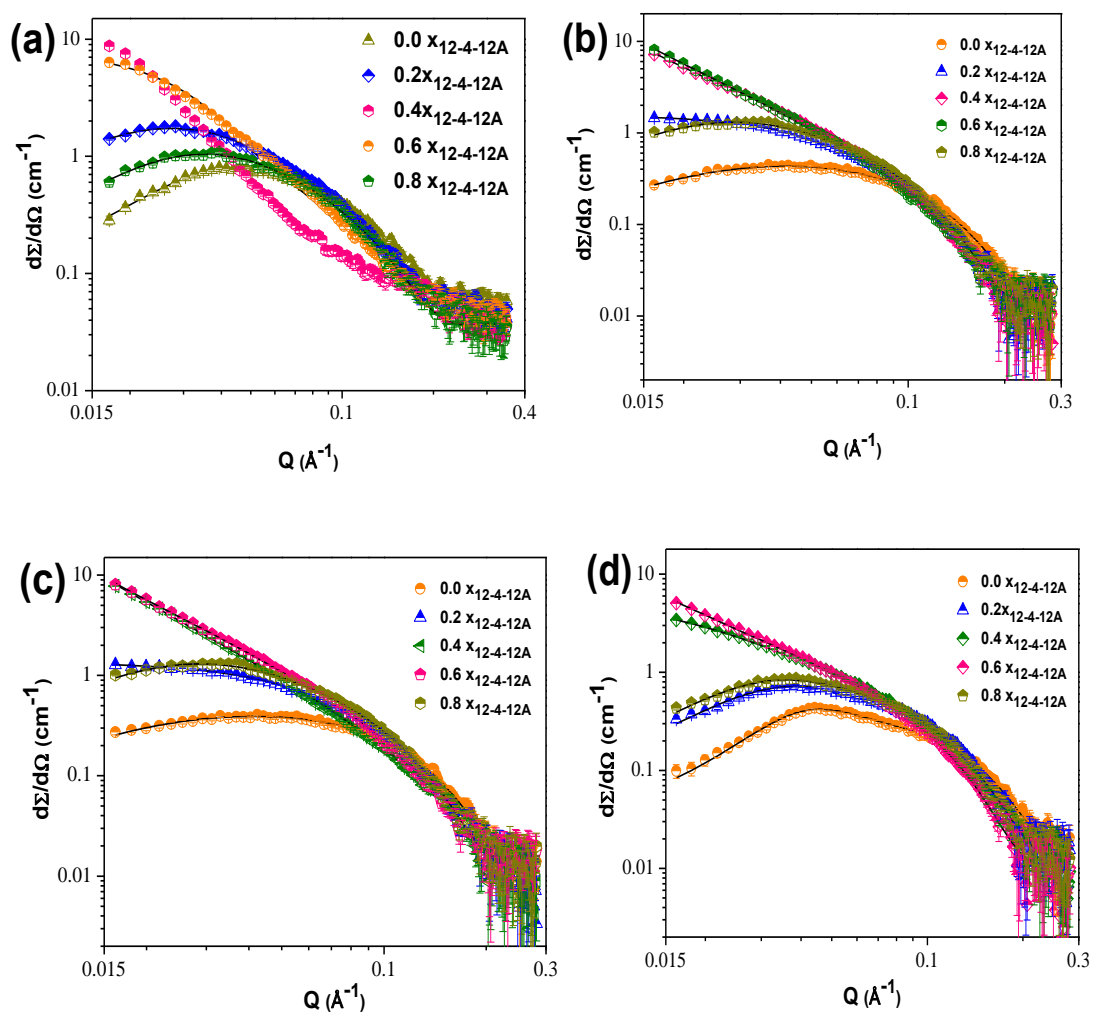


**Figure 6.** SANS spectra of 10 mM mixed aqueous gemini surfactant systems at different mole fraction of anionic gemini surfactant ( $x_{12-4-12A}$ ) at 303 K: (a) 12-4-14; (b) 12-Eg-12 (c) 12-Isb-12 and (d) 12-Eda-12.

**Table 4.** SANS fitted micellar parameters of 10 mM aqueous mixed gemini surfactant systems at 303 K

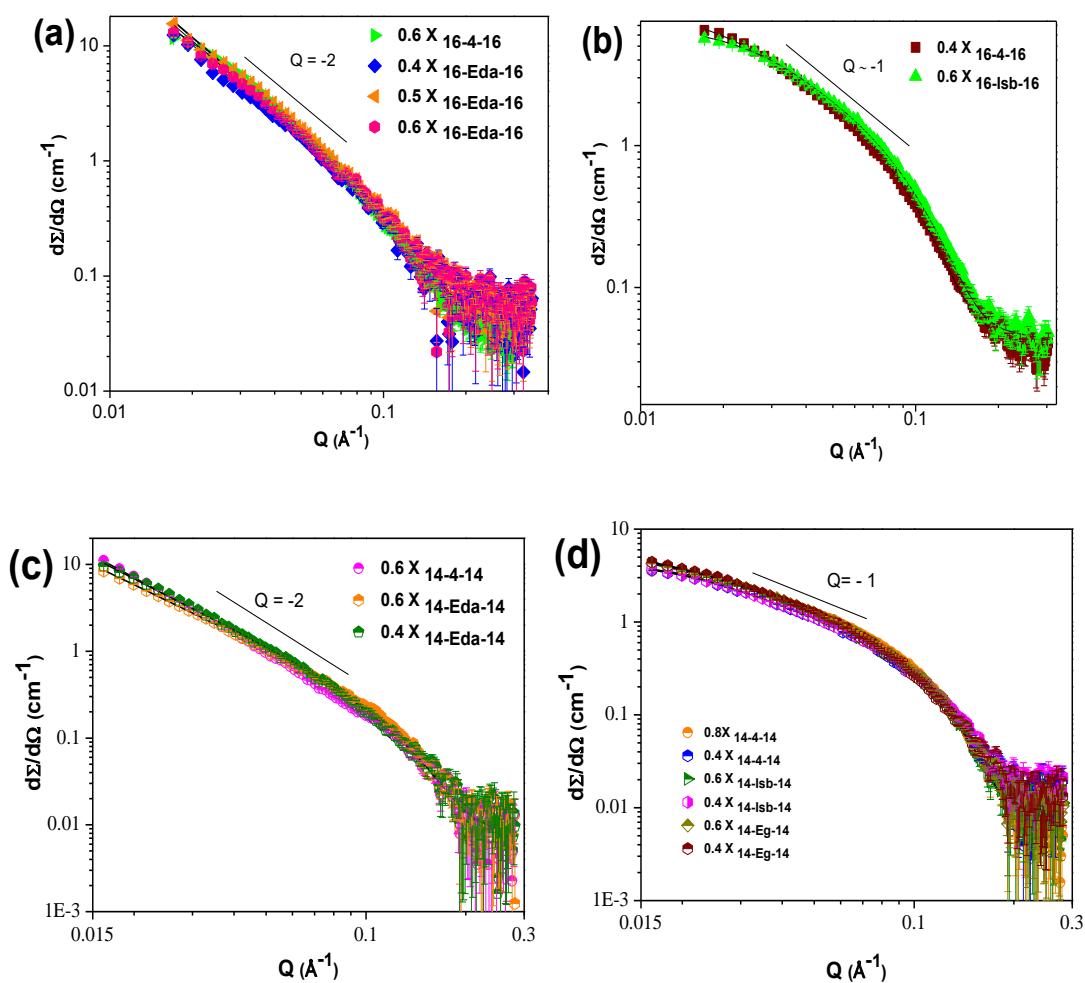
$x_{12-4-12A}$	Semi-major axis $a$ (Å)	Semi-minor axis $b$ (Å)	Fractional charge ( $\alpha$ )	Aggregation Number
<b>12-Eda-12</b>				
0.0	23.3	15.4	1.06	33
0.2	30.2	17.7	0.46	57
0.4	158.3	19.7	-	367
0.6	<b>Vesicles with a bi-layer thickness of 30.0 Å</b>			
0.8	36.1	17.6	0.4	67
1.0	29.5	14.1	0.65	35
<b>12-Eg-12</b>				
0.0	27.9	15.4	0.31	39
0.2	57.5	18.9	-	123
0.4	<b>Vesicles with a bi-layer thickness of 30.0 Å</b>			
0.6	<b>Vesicles with a bi-layer thickness of 30.0 Å</b>			
0.8	52.8	19.0	0.02	114
1.0	29.5	14.1	0.65	35
<b>12-4-12</b>				
0.0	30.0	16.3	0.53	48
0.2	67.6	17.6	0.16	125
0.4	<b>Multilamellar Vesicles with an interlayer distance of 34.7 Å</b>			
0.6	<b>Vesicles with a bi-layer thickness of 21.2 Å</b>			
0.8	44.2	17.1 Å	0.28	77
1.0	29.5	14.1	0.65	35
<b>12-Isb-12</b>				
0.0	24.8	16.6	0.28	41
0.2	52.6	18.5	-	117
0.4	<b>Vesicles with a bi-layer thickness of 30.0 Å</b>			
0.6	<b>Vesicles with a bi-layer thickness of 30.0 Å</b>			
0.8	52.0	19.3	0.2	116
1.0	29.5	14.1	0.65	35

Therefore, the polarity of the spacer has a role to play in deciding the self-assembly to be formed in an aqueous oppositely charged gemini mixture. With 14 C cationic geminis, all the systems show better growth tendencies (Table 4) than their higher chain-length counter-parts (16C, Table 3). If this trend is any hint then mixtures with equal carbon chain-length (12-s-12 and 12-4-12A) should show even better tendencies of forming higher order aggregates. Data of Table 5 distinctly show that all cationic gemini surfactant(s) (with both hydrophobic and hydrophilic spacers) have a tendency of forming higher sized rod-shaped micelles as well as vesicles on the compositions mentioned above. This unusual growth pattern (against expected lower  $P$  value with decreasing alkyl chain-length) required separate discussion. There may be a hindrance in packing when unequal carbon chains of the two components are mixed. Contrary to this, equal chain-length packing can be energetically favorable and responsible for the formation of higher order aggregates (*e.g.*, vesicles). This may be the reason for getting vesicular aggregates (bilayer or multilayer formation) with all the geminis having 12 C chain (at certain compositions).

The bi-layers are again converted to rod-shaped micelles and then to ellipsoidal ones with the further increase of the content of 12-4-12A in the mixture. Data of Figure 7 (a-f) show the characteristic  $Q$  decay for vesicles and rod-shaped micelles (a slope of -2 or -1), indicative of roles of the spacer and chain-length [22]. The vesicle bi-layer thickness can be determined from SANS data using a cross-sectional Guinier plot and the value has been found in the range 22-31 Å. The values are in good agreement with other reported surfactant systems [22, 50]. For one composition (0.4  $X_{12-4-12A}$  + 0.6  $X_{12-4-12}$ ), SANS data reveals the presence of multilamellar vesicles (Figure 8). The hump at  $Q = 0.181 \text{ \AA}^{-1}$  (Figure 8) corresponds to the Bragg peak of the repeat distance of bilayer structures in the multilamellar vesicle (MLV). Usually, the scattering from MLV in the

lower  $Q$  region follows the power law ( $1/Q^4$ ) of Porod scattering from large MLVs. The significantly slower slope ( $-3$ ) of the scattering pattern from that of Porod scattering ( $-4$ ) suggests the presence of another structure such as unilamellar vesicles as seen at a higher mole fraction of 12-4-12A (Figure 7e,  $0.6 X_{12-4-12A} + 0.4 X_{12-4-12}$ )

Above observations indicate that spacer nature, composition and chain-length compatibility play important roles in deciding the nature of higher order aggregate in aqueous solution [29, 51-53]. Morphology of aggregates is further studied by DLS and TEM to corroborate SANS data.



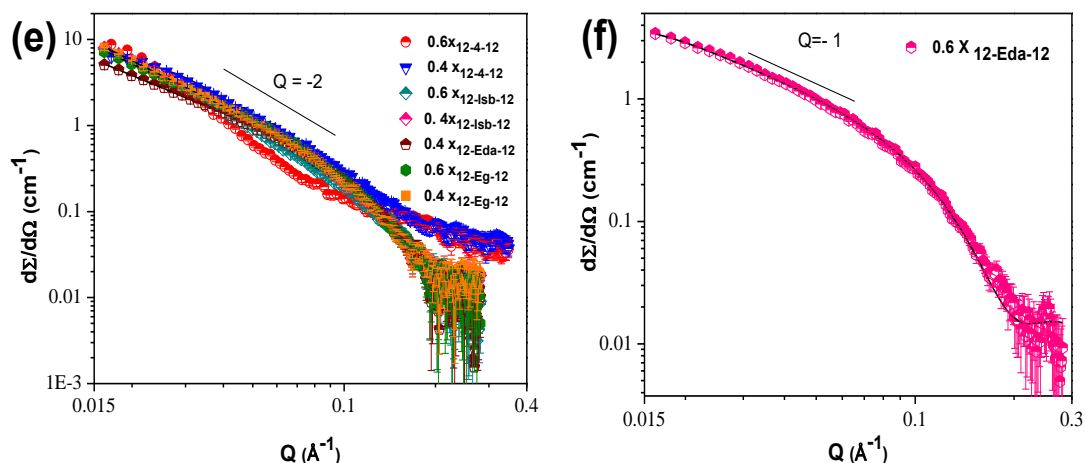


**Figure 7.** (a) SANS spectra of 10 mM aqueous mixed gemini surfactant system showing vesicular aggregates and (b) SANS spectra of 10 mM aqueous mixed gemini surfactant system having rod-shaped micelles.

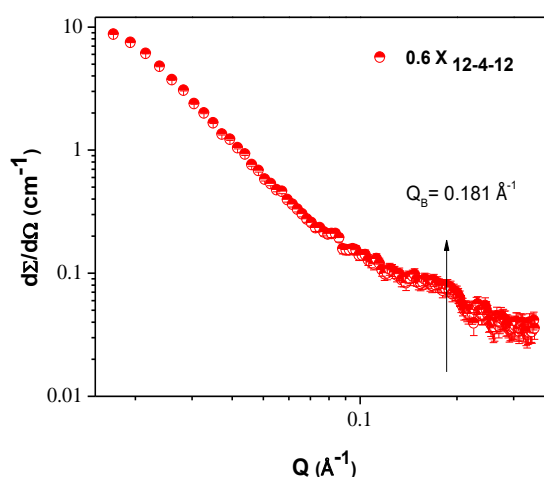


**Figure 8.** SANS spectra of 10 mM aqueous mixed gemini surfactant system showing multilamellar vesicular aggregates.

Figure 9 (a,b and c) depicts the variation of hydrodynamic diameter ( $D_h$ ) with the composition of the different mixed gemini systems. The aggregate has an average  $D_h$  value  $\sim 15$  nm for all the individual gemini surfactants. Composition variation in the mixture of any two geminis from 0.2 to 0.8-mole fraction results in structural transitions as observed from the SANS study (*vide supra*). In the composition range (0.4 to 0.6), the  $D_h$  value of the aggregate is  $\sim 65 \pm 5$  nm. However, the above size range was not observed (Figure 8 c) when the mixture contains gemini having -Eg- spacer. The

magnitude of  $D_h$  in the composition range of 0.4 to 0.6 together with the bluish color of the mixture indicates that the aggregates are vesicles whereas mixture with -Eg-spacer gemini contains ellipsoidal micelles.

However, a single major peak indicates the presence of one kind of aggregates in the system (vesicles or mixed micelles). DLS data (Figure 10), for 12-4-12 + 12-4-12A systems at the above compositions, show distinctly bigger aggregates ( $D_h = 250 \pm 30$  nm) as were observed from SANS results (Table 5). Data distinctly show the maximum change in  $D_h$  when the mixture contains nearly equal mole fractions of the two components. Overall DLS data are in consonance with SANS results and confirm the presence of higher order aggregates e.g., Vesicles.

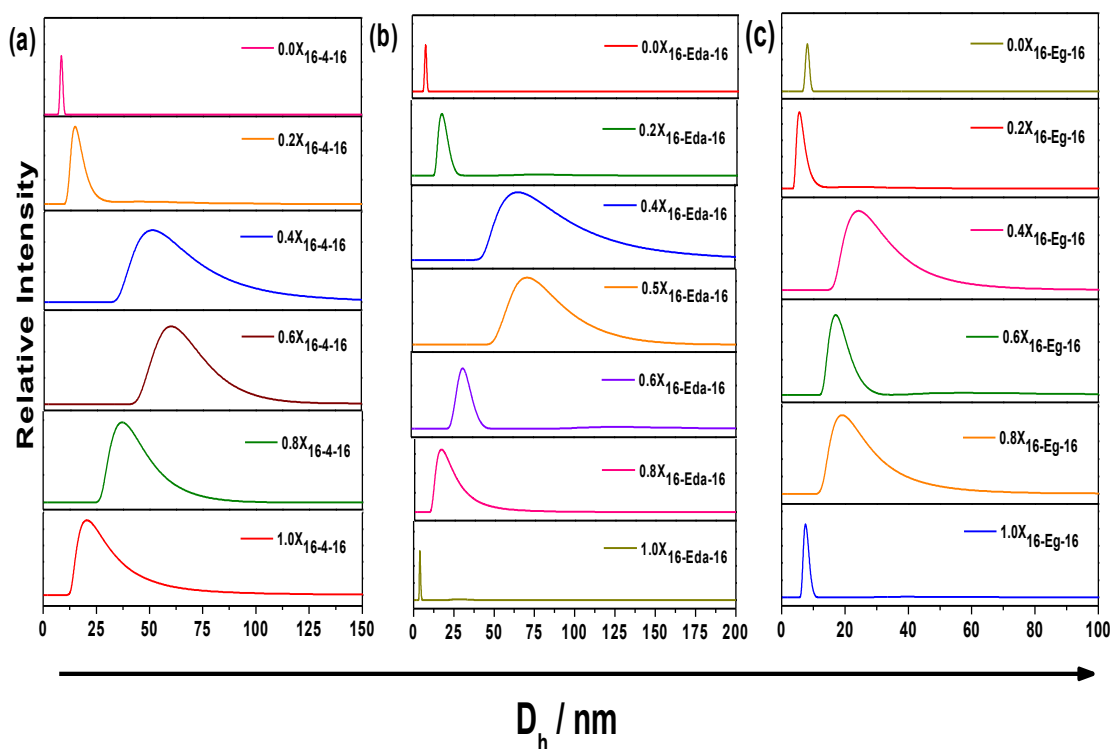


**Figure 9.** DLS data of 10 mM aqueous mixed gemini surfactant system at different mole fractions of anionic gemini surfactant ( $x_{12-4-12A}$ ) at 303 K: (a) 16-4-16; (b) 16-Eda-16 and (c) 16-Eg-16.

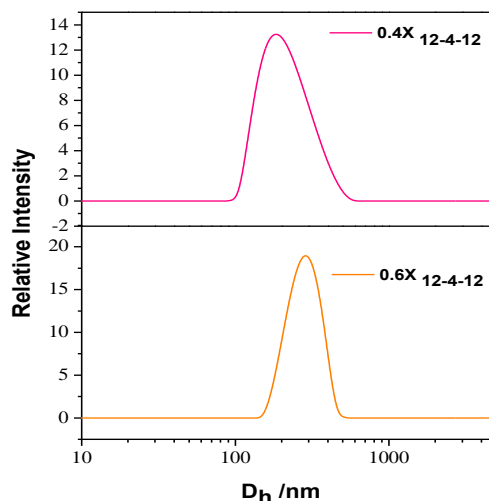


**Figure 10.** DLS data of 10 mM aqueous mixed gemini surfactant system (12-4-12 +12-4-12A) at two mole fractions of anionic gemini surfactant ( $x_{12-4-12A}$ ) at 303 K

TEM observations have also been used to support the information, regarding the formation of vesicles in the solution, obtained from SANS and DLS studies. Figures 11-13 show TEM micrographs (negatively stained) of different gemini mixtures. For gemini with polymethylene, spacer exhibits both formation of open ( $0.4 X_{16-4-16}$ ) and closed ( $0.6 X_{16-4-16}$ ) vesicles in the aqueous mixture. Due to above morphologies, SANS and DLS data were found different for the above two compositions. However, gemini with Eda spacer, in the mixture, shows the formation of closed vesicles with both the compositions ( $0.4$  or  $0.5 X_{16-Eda-16}$ ). Above data clearly, indicate that vesicle formation is dependent on both the composition and nature of the spacer. Data of Figure.13 needs special mention. This system (12-4-12A +12-4-12, 0.4 and 0.6) shows distinctly bigger vesicles than the one formed with 16-4-16 + 12-4-12A. This supports the preposition that alkyl chain packing (with equal chain components) facilitates the formation of larger aggregates. TEM images corroborate the idea of vesicle formation proposed on the basis of SANS data and DLS results.

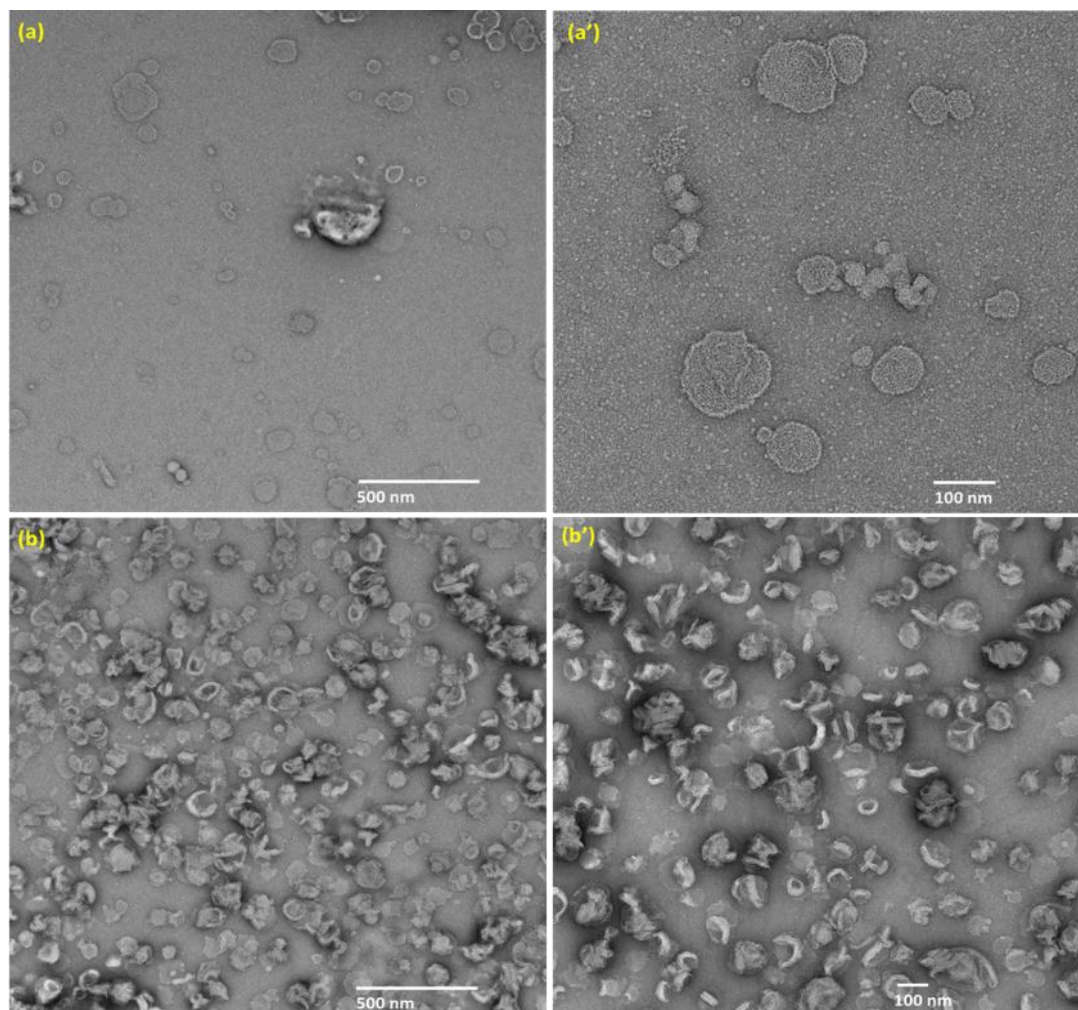


**Figure 11.** Negative stained TEM images of 10 mM mixed gemini surfactant system of 16-4-16 + 12-4-12 A (a, a')  $0.6 x_{16-4-16}$  and (b, b')  $0.4 x_{16-4-16}$  at scale 500 and 100 nm, respectively.

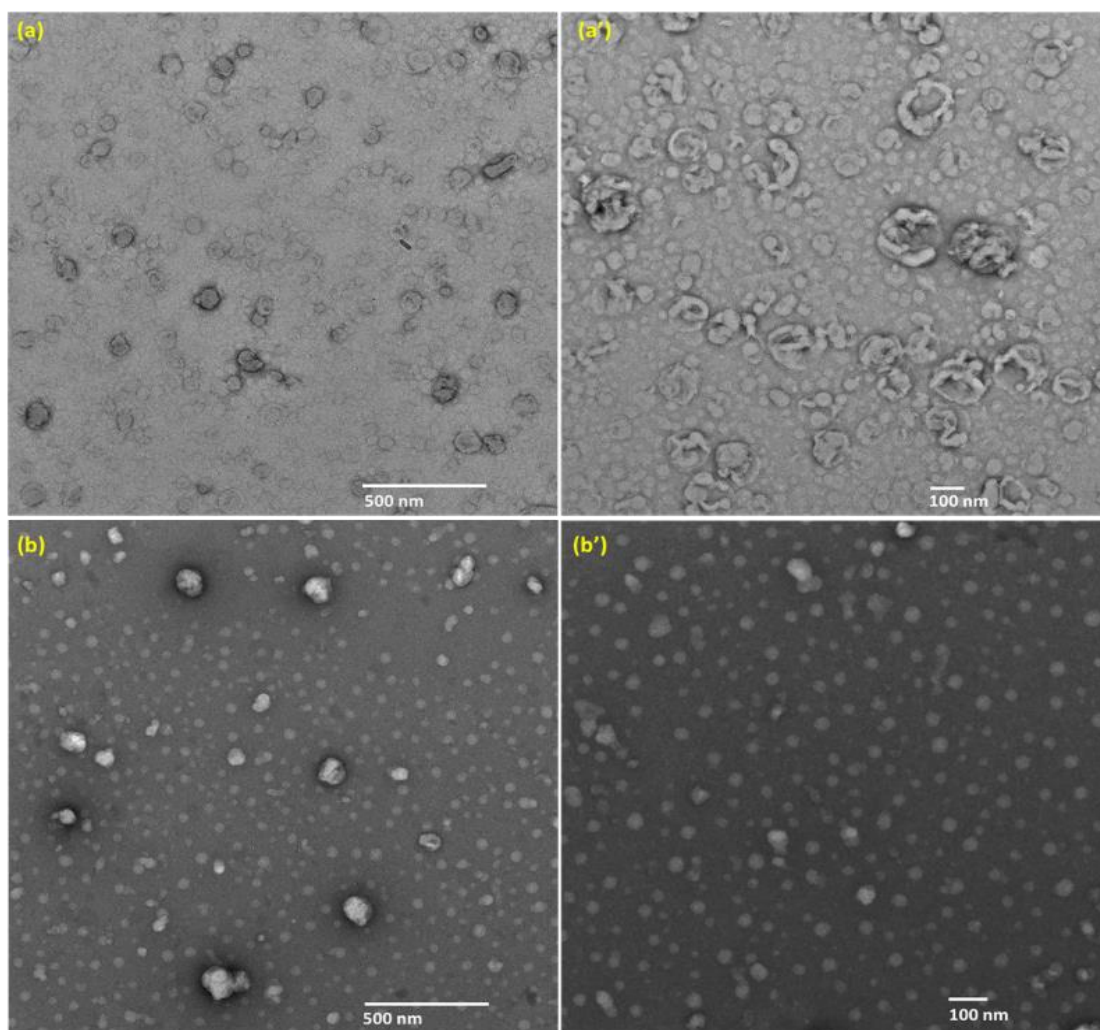


**Figure 12.** Negative stained TEM images of 10 mM mixed gemini surfactant system of 16-Eda-16 + 12-4-12 A (a, a') 0.6  $x$  16-Eda-16 and (b, b') 0.4  $x$  16-Eda-16 at scale 500 and 100 nm, respectively

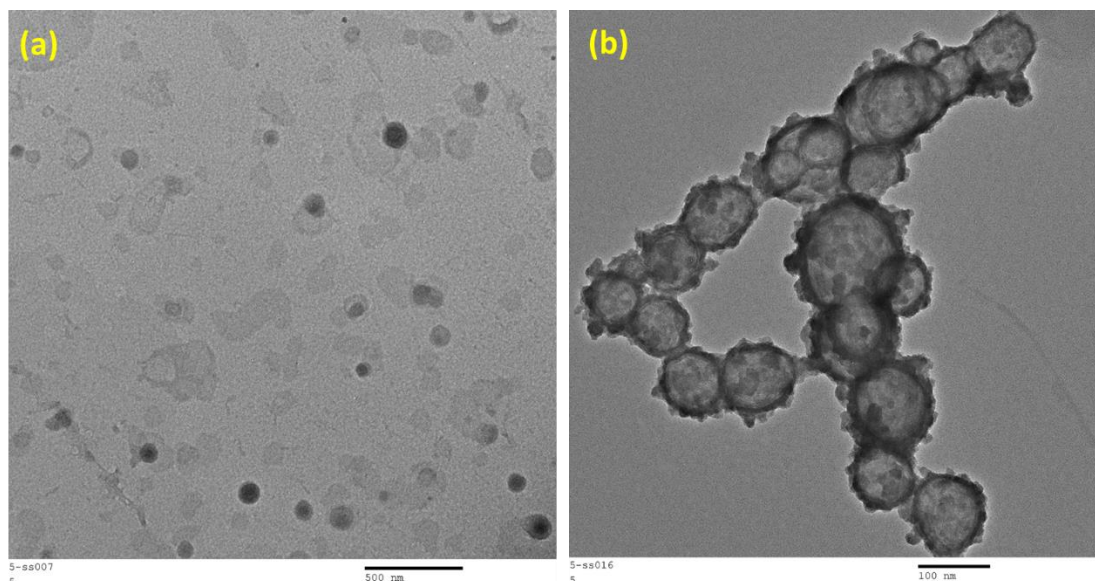


**Figure 13.** Negative stained TEM images of 10 mM mixed gemini surfactant system of 12-4-12 + 12-4-12 A ( $0.6 \times 12-4-12$ ) at scale (a) 500 nm and (b) 100 nm respectively.

### 6.2.3. Temperature Influence on Aggregate Morphologies

It has been observed that certain gemini mixtures contain vesicles at room temperature. SANS data are also acquired at different temperatures (303- 343 K) for a few mixtures (Figures 14 and 15). Overall bi-layer thickness data (Table 5) show that system with polymethylene spacer (*i.e.* 16-4-16) gives relatively stable vesicles over Eda spacer system (16-Eda-16) at equal composition. This trend was even followed with aqueous gemini mixtures of equal chain-lengths (12-4-12A +12-4-12) though having higher size aggregates. The similar insensitivity of the heating for the vesicular system has been reported recently [51]. However, a hydrophilic spacer (*e.g* Eda) may bind with background water which may release on heating and responsible for compact bilayer. In earlier studies, the morphological transition has been reported for surfactant systems with increasing temperature or shear [22, 54, 55].

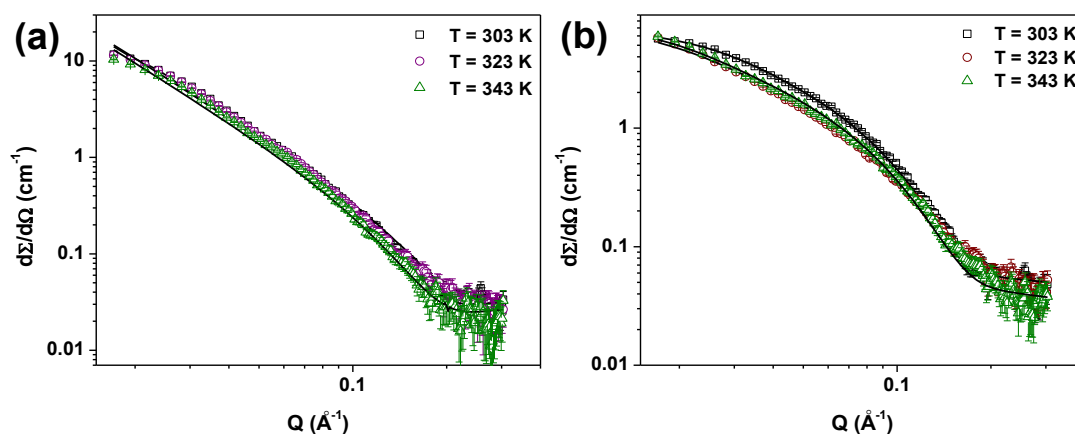


**Figure 14.** SANS spectra of 10 mM mixed gemini surfactant system (at  $0.4 x_{12-4-12A}$ ) at different temperatures ( $T$ , 303 – 343K): (a) 16-4-16; (b) 16-Isb-16.

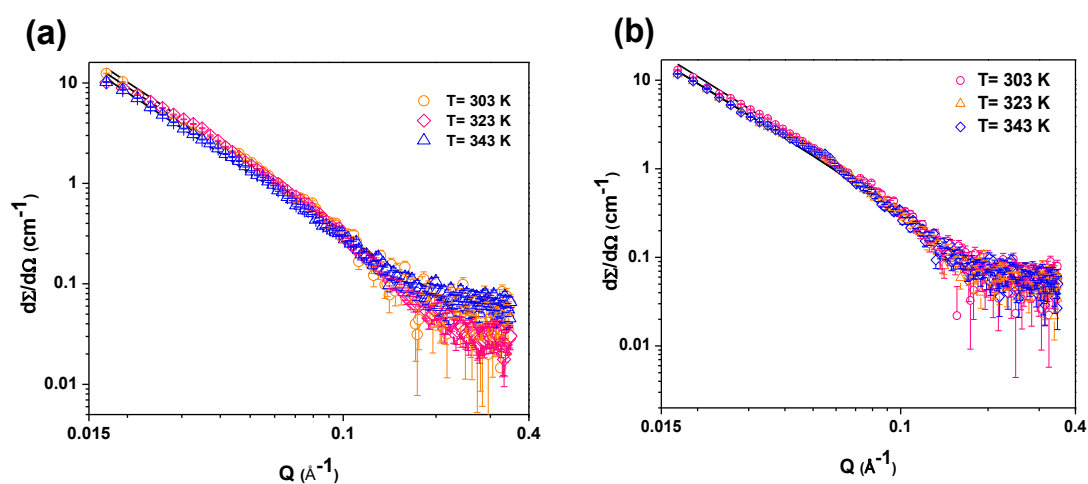


**Figure 15.** SANS spectra of 10 mM aqueous mixed gemini surfactant system (16-Eda-16 + 12-4-12A) at different mole fractions and temperature (a)  $0.4 x_{16-Eda-16}$  (b)  $0.6 x_{16-Eda-16}$

The transition has been explained on the basis of the release of oppositely charged hydrotropic counter ion from the cationic micellar surface on heating. The difference in present systems and the ones from earlier studies, [22, 54, 55] is the second component (12-4-12A) which forms mixed vesicles instead of methyl salicylate bind vesicles. A similar transition has also been observed with a cationic surfactant – alkanol system [20, 21].

**Table 5.** SANS fitted micellar parameters of 10 mM aqueous mixed gemini surfactant systems at different temperatures ( $T$ ).

$T$	$0.4 x_{16-Eda-16}$	$0.6 x_{16-Eda-16}$	$0.6 x_{16-4-16}$	$0.6 x_{16-Isb-16}$	
$K$	Bi-layer thickness ( $\text{\AA}$ )			Semi-major axis $a$ ( $\text{\AA}$ )	Semi-minor axis $b$ ( $\text{\AA}$ )
303	22.0	23.0	25.0	104.0	20.0
323	20.3	20.7	26.2	132.2	20.0
343	17.8	21.2	25.8	137.5	20.0

However, no such transition has been observed with the present system due to the fact that hydrophobic interactions (together with optimum packing) are playing a decisive role in the formation of vesicles which check the disintegration of 12-4-12A on heating. Recently, temperature induced micellar growth has also been reported in an aqueous mixture of cationic gemini with an anionic surfactant [56]. This observation of the stability of higher order aggregates on heating has not been reported many times. Our results of semi-major axis ( $b$ ), observed with -Isb- spacer gemini in the mixture ( $0.6 X_{16-Isb-16}$ ), show an increase with temperature. With heating, gradual dehydration of the oppositely charged head groups takes place which facilitates coulombic attraction. This causes a reduction in the average area of head group  $a_0$  (of resulting pseudo gemini surfactant) with a net effect of an increase in surfactant parameter value ( $P$ ) and micellar growth [48]. Therefore, aggregates of different thermal stability can be produced at will by judicious selection of the second component as well as with an appropriate spacer in two components.

### 6.3. Conclusion

The work exploits the nature of the spacer, chain-length (and composition), in a typical cationic gemini surfactant (one of the components of the oppositely charged gemini mixture), in producing structures of various morphologies. The mixing increases the surfactant packing parameter ( $P$ ), of the so-called *single surfactant* (cationic + anionic geminis). Zeta potential data show the formation of aggregates of lower charge together with charge reversal. Variations in  $P$ , spacer nature, chain-length and  $|\text{charge}|$  decide the type of the aggregates to be formed. However, composition between 0.4 to 0.6 (mole-fraction) shows moderate charge together with the formation of higher order aggregates e.g., vesicles, as observed by SANS, DLS and TEM. Influence of heating has been found to be dependent on the hydrophobic/ hydrophilic nature of the spacer. The morphologies so formed, by mixing different combinations, are exploited for the enhancement of aqueous solubility of, other-wise very less soluble organic compounds (e.g., PAH or drug, **Chapter 7**).

---

**References**

- [1] N. Kundu, D. Banik, N. Sarkar. *Langmuir*, 2018, 34, 11637-11654.
- [2] P.D. Boyer, B. Chance, L. Ernster, P. Mitchell, E. Racker, E.C. Slater, *Annu. Rev. Biochem.* 1977, 46, 955-966.
- [3] D.W. Deamer, *Microbiol. Mol. Biol. Rev.* 1997, 61,239-261.
- [4] P.L. Luisi, P. Walde, T. Oberholzer. *Curr. Opin. Colloid. interface Sci.* 1999, 4, 33-39.
- [5] S. Fleming, R.V. Ulijn, *Chem. Soc. Rev.* 2014, 43, 8150-8177.
- [6] B. György, M.E. Hung, X.O. Breakefield, J.N. Leonard. *Annu. Rev. Pharmacol Toxicol* 2015, 55, 439-464.
- [7] T.-Han Chou. S. K. Sahoo *Current Pharmaceutical Biotechnology* 16, issue 12, 2015.
- [8] L.Y. Zakharova, R.R. Kashapov, T.N. Pashirova, A.B. Mirgorodskaya, O.G. Sinyashin, *Mendeleev Commun.* 2016, 26, 457-468.
- [9] P. Yark, R. Dimova, Nanoparticle synthesis in vesicles microreactors., *InTech* 2011.
- [10] P. Tanner, P. Baumann, R. Enea, O. Onaca, C. Palivan, W. Meier. *Acc. Chem. Res.* 2011, 44, 1039-1049.
- [11] E.W. Kaler, A.K. Murthy, B.E. Rodriguez, J. Zasadzinski, *Science* 1989, 245, 1371-1374.
- [12] E.J. Danoff, X. Wang, S.-H. Tung, N.A. Sinkov, A.M. Kemme, S.R. Raghavan, D.S. English, *Langmuir* 2007, 23, 8965-8971.
- [13] X. Wang, E.J. Danoff, N.A. Sinkov, J.-H. Lee, S.R. Raghavan, D.S. English, *Langmuir* 2006, 22, 6461-6464.
- [14] L.Y. Zakhrova, A. B. Mirgorodskaya, G. A. Gayanamova, R.R. Kashapov, T. N. Pashirova, E.A. Vasilieva, Yu. F. Zuev and O.G. Sinyashin. In *encapsulations*, ed A.M. Grumezecu, Academic Press, London, 295 2016.
- [15] E.W. Kaler, K.L. Herrington, A.K. Murthy, J.A. Zasadzinski. *J.Phys. Chem.* 1992, 96, 6698-6707.
- [16] H. Yin, Z. Zhou, J. Huang, R. Zheng, Y. Zhang, *Angew. Chemie Int. Ed.* 2003, 42, 2188-2191.
- [17] W.R. Hargreaves, D.W. Deamer, *Biochem.* 1978, 17, 3759-3768.
- [18] J. Gebicki, M. Hicks, *Nature* 1973, 243, 232.

- [19] Harsha Patel Ph.D. thesis submitted to The Maharaja Sayajirao University of Baroda, 2015.
- [20] L. Sreejith, S. Parathakkat, S.M. Nair, S. Kumar, G. Varma, P.A. Hassan, Y. Talmon, *J. Phy. Chem. B*, 2010, 115, 464-470.
- [21] J. Karayil, S. Kumar, P. Hassan, Y. Talmon, L. Sreejith, *RSC Adv.* 2015, 5, 12434-12441.
- [22] T.S. Davies, A.M. Ketner, S.R. Raghavan, *J. Am. Chem. Soc.* 2006, 128, 6669-6675.
- [23] S. Lamichhane, K.B. Krishna, R. Sarukkalige, *J. environ. Manag.* 2017, 199, 46-61.
- [24] N. Fatma, M. Panda, W.H. Ansari, *Colloids Surf. A.* 2015, 467, 9-17.
- [25] Wei, J.; Huang, G.; An, C.; Yu, H. *J. Hazard Mater.* 2011, 190, 840-847.
- [26] Ansari, W. H.; Fatma, N.; Panda, M.; Kabir-ud-Din. *Soft Matter.* 2013, 9, 1478-1487.
- [27] K. Tsubone, *J. Colloid Interface Sci.* 2003, 261, 524-528.
- [28] Z. Liu, Y. Fan, M. Tian, R. Wang, Y. Han, Y. Wang. *Langmuir*, 2014, 30, 7968-7976.
- [29] X. Pei, J. Zhao, X. Wei. *J. Colloid Interface Sci.* 2011, 356, 176-181.
- [30] H. Xu, B. Liu, P. Kang, X. Bao. *J. Surf. Deterg.* 2015, 18, 297-302.
- [31] R. Zana, *Adv. Colloid. Interf. Sci.* 2002, 97, 205-253.
- [32] (a) M.J. Rosen, Gemini: a new generation of surfactants, *J. Chemtech.* 1993, 30-30. b) F. M. Menger, J. S. Keiper, Gemini Surfactants. *Angew. Chem. Int. Ed.* 2000, 39, 1906-1920.
- [33] (a) D. Kumar, N. Azum, M. A. Rub, A. M. Asiri, *J. Mol. Liq.* 2018, 262, 86-96. (b) M. A. Rub, N. Azum, F. Khan, A.M. Asiri, *J. Chem. Thermodynamics* 2018, 121, 199-210. (c) N. Azum, M. A. Rub, A. M. Asiri. *J. Dispersion Science and Technology* 2017, 38, 1785-1791. (d) M.A. Rub, N. Azum, A. M. Asiri. *J. Chemical & Engineering Data* 2017, 62, 3216-3228. (e) N. Azum, M. A. Rub, A. M. Asiri. *J. Dispers. Sci. Technol.* 2017, 38, 96-104.
- [34] W.H. Ansari, N. Fatma, M. Panda, *Soft Matter* 2013, 9, 1478-1487.
- [35] A.R. Tehrani-Bagha, H. Oskarsson, C. Van Ginkel, K. Holmberg, *J. Colloid. Interf. Sci.* 2007, 312, 444-452.

- [36] K. Parikh, B. Mistry, S. Jana, S. Gupta, R.V. Devkar, S. Kumar, *J. Mol. Liq.* 2015, 206,19-28.
- [37] H. Nakahara, H. Nishizaka, K. Iwasaki, Y. Otsuji, M. Sato, K. Matsuoka, O. Shibata, *J. Mol. Liq.* 2017, 244, 499-505.
- [38] F.M. Menger, B.N. Mbadugha, *J. Am. Chem. Soc.* 2001, 123, 875-885.
- [39] Z. Zhang, P. Zheng, Y. Guo, Y. Yang, Z. Chen, X. Wang, X. An, W. Shen. *J. Colloid Interface Sci.* 2012, 379, 64-71.
- [40] Z. Yaseen, S.U. Rehman, M. Tabish, *J. Mol. Liq.* 2014, 197, 322-327.
- [41] K. Sakai, S. Umezawa, M. Tamura, Y. Takamatsu, K. Tsuchiya, K. Torigoe, T. Ohkubo, T. Yoshimura, K. Esumi, H. Sakai, M. Abe. *J. Colloid Interface Sci.* 2008, 318, 440-448.
- [42] C. Bombelli, L. Giansanti, P. Luciani, G. Mancini. *Curr. Med. Chem.* 2009, 16, 171-183.
- [43] K. Parikh, B. Mistry, S. Jana, T. Gajaria, S. Gupta, R. V. Devkar, S. Kumar. *Colloid Polym. Sci.* 2015, 293, 1437-1446.
- [44] S. Kumar, K. Parikh. *J. Surf. Deterg.* 2013, 16, 739-749.
- [45] S. Singh, A. Bhadoria, K. Parikh, S.K. Yadav, S. Kumar, V.K. Aswal and S. Kumar, *J. Phy. Chem. B*, 2017, 121, 8756-8766.
- [46] S. Kumar, V. Aswal, H. Singh, P. Goyal, *Langmuir* 1994, 10, 4069-4072.
- [47] L.L. Brasher, K.L. Herrington, E.W. Kaler, *Langmuir* 1995, 11, 4267-4277.
- [48] J.N. Israelachvili, D.J. Mitchell, B.W. Ninham, *J. Chem. Soc. Faraday Transactions 2.* 1976, 72, 1525-1568.
- [49] Z. Lin, J. Cai, L. Scriven, H. Davis, *J. Phy.Chem.* 1994, 98, 5984-5993.
- [50] H. Jung, B. Coldren, J. Zasadzinski, D. Iampietro, E. Kaler, Proceedings of the National Academy of Sciences 98(4) (2001) 1353-1357.
- [51] S. Rajkhowa, S. Mahiuddin, J. Dey, S. Kumar, V. Aswal, R. Biswas, J. Kohlbrecher, K. Ismail, *Soft matter* 2017, 13, 3556-3567.
- [52] V.K. Bansal, D.O. Shah, J.P. O'Connell. *J. Colloid. Interf. Sci.* 1980, 75, 462-475
- [53] L.S. Hao, J. Wu, Y.R. Peng, Y. Wang, K. Xiao, Y. Hu, and Y.Q. Nan, *Langmuir*, 28, 34, 7319-7333.
- [54] R.T. Buwalda, M.C. Stuart, J.B. Engberts, *Langmuir* 2000, 16, 6780-6786.

[55] Y. Zheng, Z. Lin, J. Zakin, Y. Talmon, H. Davis, L. Scriven, *J. Phy. Chem. B* 2000, 104, 5263-5271.

[56] X. Ji, M. Tian, Y. Wang, *Langmuir* 2016, 32, 972-981.